III-N-V low-bandgap nitrides and their device applications

2001 J. Phys.: Condens. Matter 13 7169

(http://iopscience.iop.org/0953-8984/13/32/319)

INSTITUTE OF PHYSICS PUBLISHING JOURNAL OF PHYSICS: CONDENSED MATTER

J. Phys.: Condens. Matter **13** (2001) 7169–7182 PII: S0953-8984(01)25592-1

III–N–V low-bandgap nitrides and their device applications

C W Tu

Department of Electrical and Computer Engineering, University of California, San Diego La Jolla, CA 92093-0407, USA

Received 7 June 2001, in final form 7 June 2001
Published 26 July 2001
Online at stacks.iop.org/JPhysCM/13/7169

Abstract

Four families of III–N–V compounds for electronic and optoelectronic applications are presented: InNAsP/InP, GaInNAs/GaAs, Ga(In)NP/GaP and GaInNP/GaAs. InNAsP/GaInAsP quantum wells grown on InP are superior for long-wavelength microdisc lasers (and so expected for edge-emitting lasers), as compared to GaInAs/GaInAsP quantum wells, because of the larger conduction band offset from the addition of a small amount of nitrogen (0.5% to 1%) in the InAsNP quantum wells. GaInNAs/GaAs heterostructures emitting at 1.3 μm at room temperature have stimulated much interest in 1.3 μm vertical-cavity surface-emitting lasers. Here we report the use of GaInNAs as the base of a heterojunction bipolar transistor (HBT), which exhibits a lower turn-on voltage than HBTs with the usual GaInAs base. Incorporating a small amount of N in GaN_xP_{1-x} alloys leads to a direct bandgap behaviour of GaNP, and red light-emitting diodes based on a GaNP/GaP double heterostructure grown directly on (100) GaP substrates have been fabricated. Finally, incorporating N into GaInP barriers in a quantum well is shown to lower the conduction band offset, and GaInNP/GaAs could be potentially ideally suited for npn HBTs.

1. Introduction

Recently there has been much interest in III–N–V compound semiconductors, because only a small amount of nitrogen incorporation (∼2%) in conventional GaAs- and InP-based III–V compounds results in very large bandgap bowing [1, 2]. This allows 1.3 μm to 1.55 μm light emission at room temperature from GaInNAs/GaAs quantum wells (QWs) and quantum dots (QDs), described in section 3. Low-bandgap GaInNAs can also be used as the base of a hetero-junction bipolar transistor (HBT) to obtain a low turn-on voltage for low-power applications, discussed in section 4. Furthermore, because of the large electronegativity of N atoms, N incorporation pulls down the conduction band and valence band edges, leading to a larger conduction band offset, which has many advantages for device applications. Examples are

InNAsP/GaInAsP QW microdisc lasers, described in section 2, and GaInNP/GaAs as a possible ideal material for HBTs, described in section 6. N incorporation can also change the band structure of the host material, e.g., from indirect bandgap to direct bandgap, as in the case of GaNP/GaP, from which light-emitting diodes (LEDs) were fabricated, as described in section 4.

2. InNAsP/InP

Long-wavelength lasers emitting at 1.3 and 1.55 μm are important for optical-fibre communications and have been intensively investigated. These lasers were commonly realized with the GaInAsP–InP material system, but they have poor performance at high temperature (25 °C to 85 °C) and thermoelectric coolers are often required for their use in optical-fibre communication systems. The high-temperature performance is described by a characteristic temperature T_0 where the temperature dependence of the threshold current density is proportional to $\exp(T/T_0)$. Obviously, a higher T_0 is desirable. In the case of the GaInAsP–InP system, To is about 60 K, due to the small conduction band offset resulting in poor electron confinement in the QWs [3]. (The hole confinement is less of a problem because of heavier effective hole masses.) Materials with a larger conduction band offset and a higher T_0 have been reported, e.g., the AlGaInAs/InP system with a T_0 of 105–120 K [4] and the AlGaInAs/InAsP system with a T_0 of 116 K [5]. In 1995 Kondow *et al* proposed a novel material system, GaInNAs/GaAs [2], and they reported a T_0 of 126 K for a laser emitting at 1.2 μm [6]. GaInNAs/GaAs vertical-cavity surface-emitting lasers (VCSELs) emitting at 1.3 μm are also actively pursued because one can use the GaAs/AlGaAs distributed Bragg reflector (DBR) mirrors [7, 8]. In this section we describe another Al-free material system for long-wavelength lasers at 1.3 and 1.55 μm: InNAsP/InP [9].

We have grown N-containing III–V ternaries and quaternaries by gas-source molecular beam epitaxy with an RF plasma nitrogen radical beam source, elemental group III sources and cracked arsine and phosphine. Despite the low solubility limits of N in arsenides and phosphides [10], the highest N composition we have obtained in InNP is 1% [11], whereas that in GaNP [12] and GaNAs [13] is 16%. These numbers are the highest reported to date. Figure 1 shows the bandgap as a function of nitrogen concentration in InNP [11]. The dashed line is a linear interpolation between InP and InN. At small concentration range, the bandgap bowing agrees with the calculations based on the Van Vechten model [14], which is a perturbation theory.

Because nitrogen has a large electronegativity [15], incorporating nitrogen into the

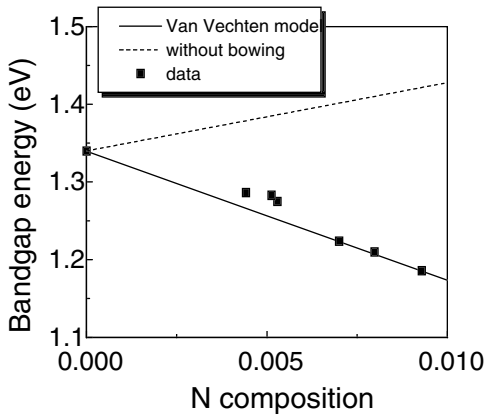

Figure 1. Bandgap energy of InNP as a function of N concentration. The bandgaps were measured by absorption spectroscopy [11].

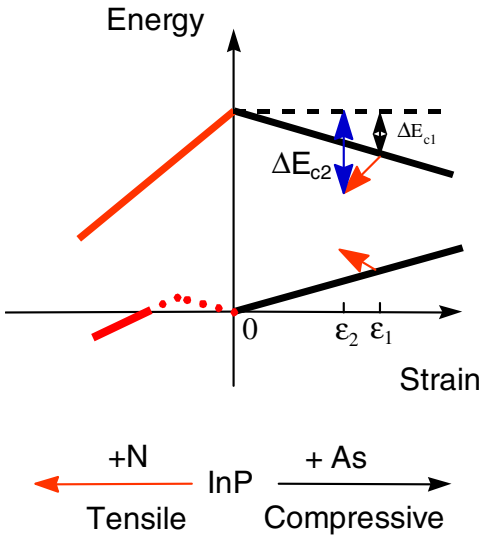

Figure 2. Conduction band and valence band edges for InAsP and InNP.

conventional III–V materials pulls down both conduction-band and valence-band edges, resulting in a larger conduction-band offset. Figure 2 shows qualitatively the band edges for InAsP and InNP as a function of strain. Adding As into InP increases the lattice constant, resulting in compressive strain in the plane parallel to the interface. The bandgap becomes smaller; the conduction band edge moves down and the valence band edge moves up. On the other hand, adding N to InP results in tensile strain and smaller bandgap. From linear interpolation of the large electronegativity of nitrogen, we expect the valence band edge to move down with nitrogen incorporation. Experimental evidence, however, from cross-section scanning tunnelling microscopy of the filled states of InP, InAsP and InNAsP indicates that the valence band edge of InNAsP is higher than that of InAsP [16]. The important point is that adding N to a compressive-strained layer reduces the strain from ε_1 to ε_2 and increases the conduction band offset from ΔE_{c1} to ΔE_{c2}, resulting in better electron confinement.

Figure 3 shows the effect of N incorporation in InAsP. Curve (a), the bottom one, is a high-resolution x-ray rocking curve for an InAsP/InP MQW, and curve (b) is for a similar sample with some nitrogen incorporation. We see that the superlattice satellite peaks become sharper, indicating better structural quality, but, more importantly, the envelope of the satellite peaks shifts toward the substrate peak, indicating less strain. By adding different amounts of nitrogen, we can obtain different emission wavelengths, e.g., 1.3 μm and 1.5 μm.

Figure 4(a) shows the microdisc laser structure, which consists of just a 1.3 μm single quantum well (SQW) of InNAsP/GaInAsP grown on InP, and figure 4(b) shows a fabricated microdisc with a diameter of 5 μm [17]. The mesa is first defined by reactive ion etching to the InP layer, followed by wet chemical etching, which is isotropic and etches InP but not GaInAsP. Therefore, the SQW disc sits on top of an InP post as shown in figure 4(b).

Optical pumping, with a 1% duty cycle, at a wavelength of 514 nm from an argon-ion laser was then used to achieve lasing. Lasers operate up to 340 K, above the previously achieved 220 K of a 1.45 μm GaInAs/GaInAsP microdisc laser with a similar structure grown and fabricated by us. Figure 5 shows the pump threshold as a function of temperature, indicating a T_0 of 97 K, above the 60 K achieved with a GaInAs/GaInAsP microdisc laser.

Figure 6 shows the pump–light intensity plots for (a) InNAsP/GaInAsP and

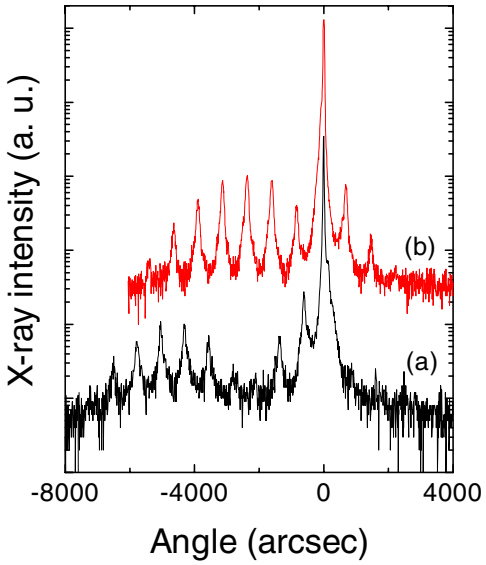

Figure 3. High-resolution x-ray rocking curves for (a) $InAs_{0.4}P_{0.6}$/InP and (b) $InNxAs_{0.4}P_{0.6-x}$/InP MQWs [9].

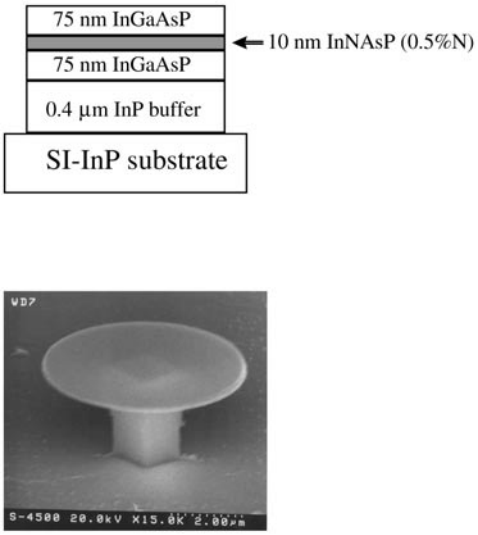

Figure 4. (a) Schematic layer structure of the InNAsP/GaInAsP microdisc laser shown in (b) [17].

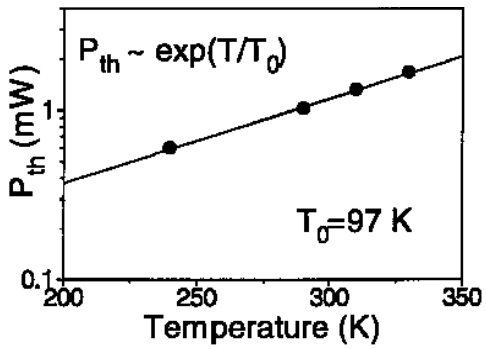

Figure 5. Laser pump threshold as a function of temperature.

(b) GaInAs/GaInAsP microdisc lasers at 85 K. At this temperature, the threshold pump power of (a) is about 20 μW, compared to the 36 μW of (b). Furthermore, the emission intensity saturates in (b), but not in (a). These results all indicate a larger conduction band offset in the InNAsP/GaInAsP system.

3. GaInNAs/GaAs QWs and QDs

Because adding N into GaInAs decreases photoluminescence (PL) intensity rapidly [18], our approach is to use as large an In concentration as possible and as small an N concentration as possible without generation of misfit dislocations. Thus, we are in the regime of self-assembled quantum dots.

1.3 μm laser emission on GaAs has been actively pursued recently because the GaAs technology is more mature than the InP technology currently used and because GaAs/AlAs

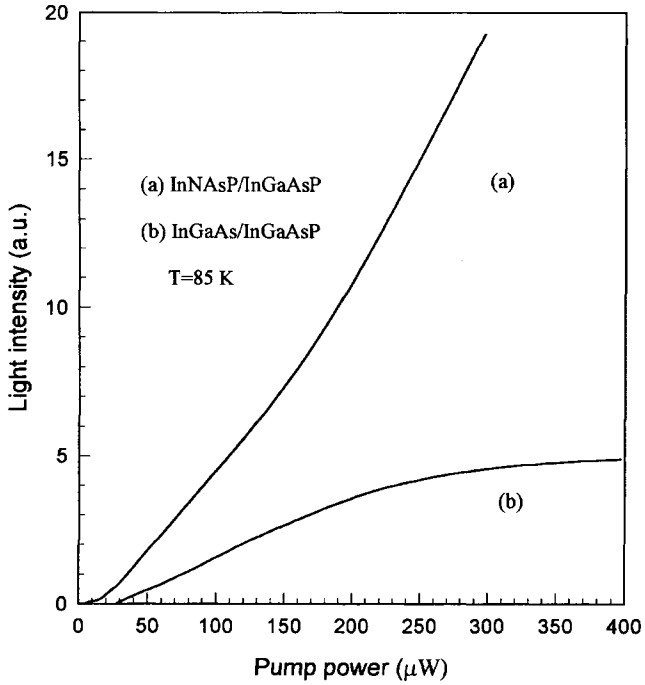

Figure 6. Output light intensity versus pump power for 5 mm diameter (a) InNAsP/GaInAsP and (b) GaInAs/GaInAsP microdisc lasers measured at 85 K [17].

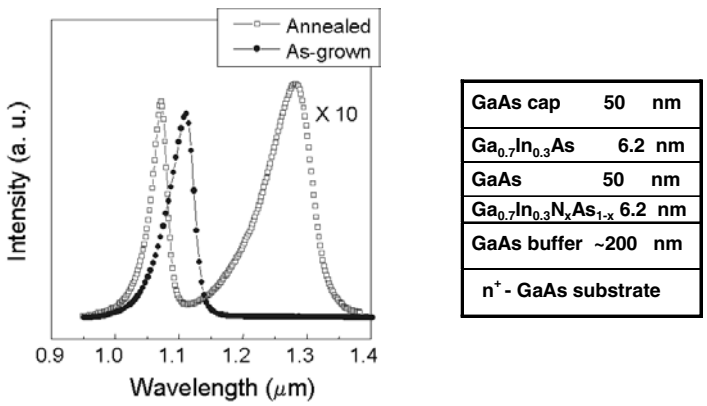

Figure 7. PL of GaInAs/GaAs and GaInNAs/GaAs SQW.

DBRs can be used in a single epitaxial growth without the need for wafer bonding of GaAs- and InP-based structures. Several approaches have been employed: self-assembled GaInAs QDs [19], GaAsSb/GaAs QWs [20, 21], GaInAs/GaPAsSb QWs [22], and GaInNAs QWs as the active layer [2]. Figure 7 shows our GaInNAs/GaAs SQW emitting at 1.3 μm, after RTA at 700 °C [23]. As-grown samples show no PL at room temperature.

To extend the wavelength longer, to 1.55 μm emission, our approach is to grow GaInNAs QDs [24]. Since we know that the more the nitrogen is incorporated, the lower the PL intensity, we use high In concentration (in this case 70%) and low nitrogen concentration

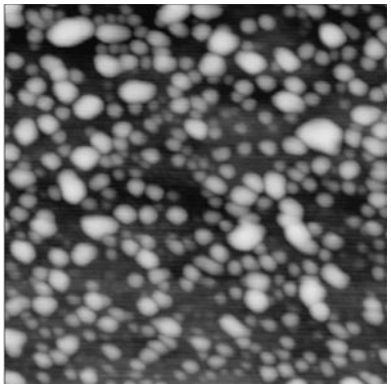

Figure 8. AFM image of a 5.5 ML $Ga_{0.3}In_{0.7}N_{0.04}As_{0.96}$ QD grown at 450 °C. The image size is 0.5 μm × 0.5 μm [25].

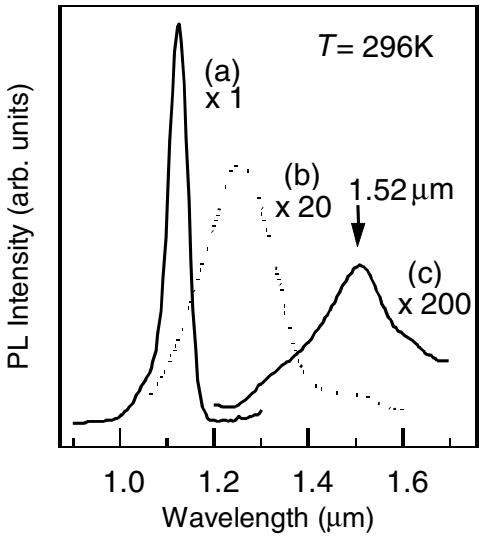

Figure 9. Room-temperature PL spectra from 4 ML (a) $Ga_{0.3}In_{0.7}As$ and (b) $Ga_{0.3}In_{0.7}N_{0.02}As_{0.98}$ QD grown at 520 °C and (c) 5.5 ML $Ga_{0.3}In_{0.7}N_{0.04}As_{0.96}$ QD grown at 420 °C [24].

(4%). Therefore, we are in the GaInAs QD regime on GaAs. The sample structure consists of a 150 nm thick GaAs buffer layer grown at 580 °C on a GaAs substrate, one layer of GaInNAs islands, a 50 nm thick GaAs barrier layer and finally a second layer of GaInNAs islands using growth parameters similar to the first layer. The optimal growth temperature for QDs turns out to be 420–450 °C. A transition from two-dimensional to three-dimensional growth mode, i.e., Stranski–Krastanov growth mode, is confirmed as the reflection high-energy electron diffraction pattern transforms from streaks to chevrons at the nominal thickness of approximately 3 monolayers (MLs).

Figure 8 shows an atomic force microscopy (AFM) image of a 5.5 ML $Ga_{0.3}In_{0.7}N_{0.04}As_{0.96}$ QD grown at 450 °C. Each side is 0.5 μm. The compositions are nominally what they would be in a GaInNAs quantum well grown with similar RF power and fluxes at 460 °C. The island density, $\sim 1 \times 10^{11}$ cm^{-2}, decreases and the island size, ∼30 nm at the base by ∼10–15 nm in height, increases with increasing growth temperature, as observed in other material systems. Figure 9 shows room-temperature PL spectra from three GaIn(N)As QD samples indicating that the peak wavelength can be tuned at least from 1.10 to 1.52 μm. Figures 9(a) and (b) show, respectively, PL spectra from $Ga_{0.3}In_{0.7}As$ and $Ga_{0.3}In_{0.7}N_{0.02}As_{0.98}$ QD grown with 4 ML at 520 °C (the nitrogen concentration is actually less because the growth temperature is higher than 460 °C). Figure 9(c) shows the PL of 5.5 ML $Ga_{0.3}In_{0.7}N_{0.04}As_{0.96}$ QD's grown at 420 °C. The integrated intensity is about a factor of ten larger near 1.3 μm than near 1.55 μm. This is one of the first reports extending GaInNAs emission to 1.5 μm.

4. $Ga_{0.89}In_{0.11}N_{0.02}As_{0.98}$/GaAs HBTs

GaAs-based HBTs have achieved widespread use in high-performance microwave and digital applications. They have, however, a large base-emitter turn-on voltage of approximately 1.4 V

(at high current density), which is awkward for use in circuits with low power supply voltage. It is, therefore, important to develop techniques to reduce the value of the turn-on voltage for low-power applications. The turn-on voltage is related to the bandgap of the base. In this section, we describe our investigation using GaInNAs as the base of an HBT [25].

Table 1. A GaInNAs-base HBT structure [25].

Layer	Material	Thickness (nm)	Doping (cm^{-1})
Cap	GaAs	200	$n = 5 \times 10^{18}$
Emitter	GaAs	200	$n = 5 \times 10^{17}$
δ doping	GaAs	0.5	$n = 3 \times 10^{19}$
Graded	GaAs⇐	30	$n = 3 \times 10^{17}$
	$Ga_{0.89}In_{0.11}N_{0.02}As_{0.98}$	30	
Spacer	$Ga_{0.89}In_{0.11}N_{0.02}As_{0.98}$	5	undoped
Base	$Ga_{0.89}In_{0.11}N_{0.02}As_{0.98}$	40	$p = 8 \times 10^{18}$
Spacer	$Ga_{0.89}In_{0.11}N_{0.02}As_{0.98}$	5	undoped
Graded	$Ga_{0.89}In_{0.11}N_{0.02}As_{0.98}$ ⇐ GaAs	30	$n = 3 \times 10^{16}$
δ doping	GaAs	5	$n = 1.5 \times 10^{18}$
Collector	GaAs	400	$n = 3 \times 10^{16}$
Sub-collector	GaAs	700	$n = 5 \times 10^{18}$
S.I. GaAs substrate			

Table 1 shows a schematic layout of the GaInNAs-base HBT structure. Since most of the bandgap lowering from nitrogen incorporation is a result of lowering of the conduction band edge [26], nitrogen incorporation results in an increase of the conduction band discontinuity for GaInNAs/GaAs. Grading and delta doping layers (interface doping dipole) were designed to eliminate the barriers at the base–emitter and base–collector junctions. The grading between GaAs and $Ga_{0.89}In_{0.11}N_{0.02}As_{0.98}$ was done with a $Ga_{0.89}In_{0.11}N_{0.02}As_{0.98}$/GaAs chirped superlattice with a period of 1.1 nm to make sure the electrons can tunnel through the barriers. The $Ga_{0.89}In_{0.11}N_{0.02}As_{0.98}$ base is 40 nm thick with a nominal doping of 8×10^{18} cm^{-3}.

The HBTs were fabricated using a self-aligned process. All measurements were made on a device with a 120×120 μm^2 emitter. The ideality factor for the base–collector junction is 1.05, indicating near ideal collector current. The ideality factor for the base–emitter junction, however, is 1.59, indicating a substantial space-charge recombination current. Figure 10 shows a comparison of the collector current for a $Ga_{0.89}In_{0.11}N_{0.02}As_{0.98}$ base HBT with a conventional GaAs HBT with a base doping of 4×10^{19} cm^{-3} and AlGaAs grading between the base–emitter junction. The large series resistance from the low base doping limits the $Ga_{0.89}In_{0.11}N_{0.02}As_{0.98}$ base HBT when the base–emitter bias is greater than 0.7 V. The $Ga_{0.89}In_{0.11}N_{0.02}As_{0.98}$ base HBT shows a 0.4 V reduction in the turn-on voltage, compared with the GaAs base HBT.

5. Ga(In)NP/GaP

It is well known that at very low concentrations, in the 10^{16} cm^{-3} range, an isolated nitrogen introduces a highly localized state in GaP, where the energy level is located slightly below the conduction band minimum. Even though GaP is an indirect bandgap material, such spatial localization means the wavefunction has contributions from the whole k-space and leads to quasi-direct transitions in GaP:N. Thus, GaP:N has been a widely used material for green LEDs. With slightly increasing N concentrations, N forms NN pairs, which shift light

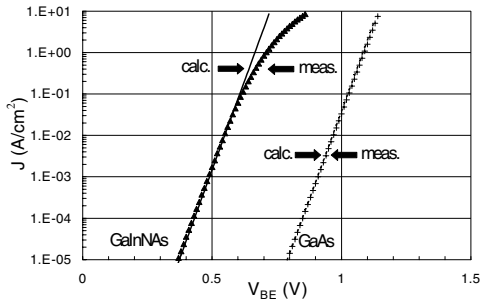

Figure 10. Comparison of the collector current for a GaInNAs base HBT with a GaAs base HBT [25].

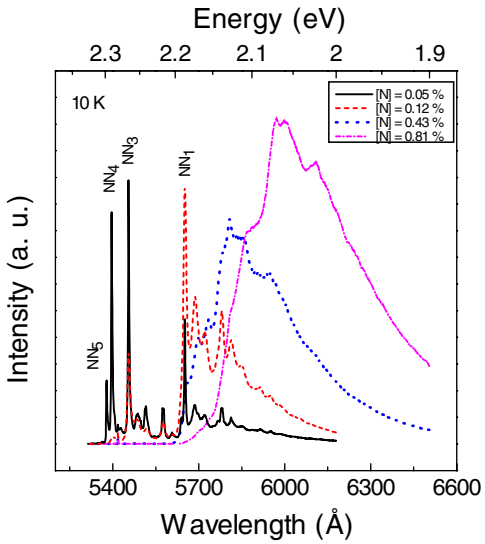

Figure 11. 10 K PL spectra of 250 nm thick GaN_xP_{1-x} with $x \leqslant 0.81\%$ [28].

emission wavelength from green to yellow. With even higher N concentration, GaNP alloys are formed. A change in the band structure of GaNP with a small amount of N incorporation has been predicted by Bellaiche *et al*, who, using 512-atom supercell pseudopotential band structure calculation, predicted the indirect–direct crossover at 3% N [27]. As reported below, we observe this cross over at an even lower N concentration.

Figure 11 shows PL spectra of 250 nm thick GaN_xP_{1-x} with $x \leqslant 0.81\%$ at 10 K [28]. For the very-low-N concentration sample ($x = 0.05\%$, corresponding to 10^{19} cm^{-3}), there are a series of sharp emission lines from different NN_i ($i \leqslant 5$) pairs, similar to previous reports [29–31]. With increasing N concentration up to 0.43%, the sharp emissions from NN_i pairs disappear and a broad PL peak with strong intensity from the GaNP alloy appears. The PL peak red-shifts, and the intensity also increases with increasing N concentration.

The room-temperature PL intensity of GaNP bulk layers increases with increasing N concentration, up to 1.3%, similar to the report of Baillargeon *et al* [32]. The PL intensity increases with higher N concentration mainly due to the increased matrix element for the transition from the conduction band to the valence band. With an N concentration more than 1.3%, PL intensity decreases due to decreased sample quality partly as a result of increased

strain relaxation.

Our results qualitatively agree with the theoretical calculation of Bellaiche *et al*, where they found a transition point from indirect to direct bandgap at an N concentration of 3% for GaNP [12]. We attribute the large bandgap reduction to the formation of a nitrogen-related impurity band evolved from nitrogen pair bound states in heavily doped GaP [33]. The inter-centre interactions or the formation of large nitrogen clusters lead to band edge states extending to the energy region below that of the lowest bound state NN_1, and thus a further reduction of the bandgap of the alloy, inducing the formation of a direct bandgap. Therefore, a very strong PL emission is expected in GaNP bulk layers. No RT PL emission was reported previously in GaNP alloys with similar N compositions, probably due to poor sample quality, not the indirect nature of the band structure.

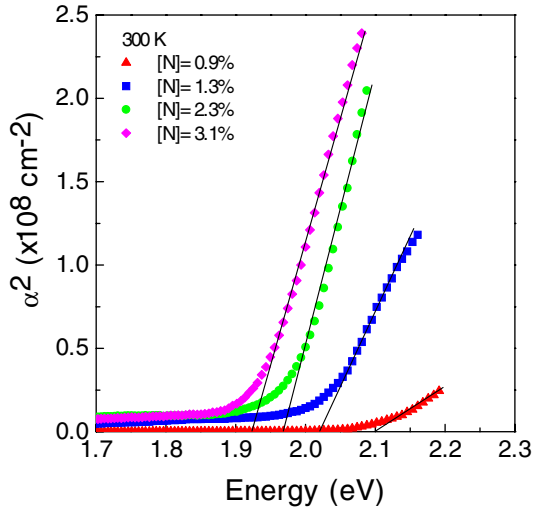

Figure 12. Square of the absorption coefficient of GaN_xP_{1-x} films as a function of photon energy [28].

Figure 12 shows the square of the absorption coefficient of GaN_xP_{1-x} films as a function of photon energy. Quite obviously, the absorption coefficient obeys a square law, indicating a direct bandgap behavior of GaNP. Furthermore, as the N concentration is increased, the band edge of GaNP shifts to lower energy, indicating a reduction of bandgap energy. To confirm the direct-bandgap nature, we have the samples characterized by pressure-dependent PL. Figure 13 shows PL transition energies as a function of applied hydrostatic pressure for samples with three different alloy compositions [34]. Two extreme cases of the pressure dependence of the indirect bandgap of GaP are also shown. It is well known that the indirect bandedge X_C shifts to lower energy with increasing pressure for all III–V semiconductors. The positive pressure coefficients of GaNP samples, on the other hand, confirm the direct bandgap nature.

We have fabricated LEDs from GaNP (1.1% N) pn homojunctions [35] as well as from GaP/GaNP/GaP double heterostructures (DHs), shown in figure 14 [36]. Electroluminescence at room temperature (RT) peaks at 670 nm, as shown in figure 15, and the results are very encouraging. The DH LEDs are 20 times more intense than pn homojunction LEDs. Because the structures were grown on lightly doped n-type GaP substrates, instead of a heavily doped one, and there was no thick GaP window layer on the top, current spreading is a problem. Although the quantum efficiency (∼1–2%) is still an order of magnitude lower than that of high-brightness AlGaInP/GaAs LEDs, the structure and the active layer is not optimized. As

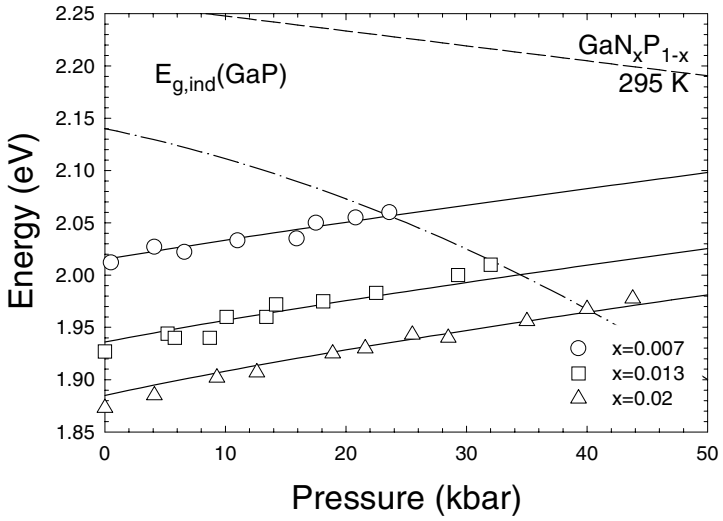

Figure 13. The pressure dependence of the PL emissions from GaN_xP_{1-x} samples with $x = 0.007$, 0.013 and 0.02. The dashed and dash–dotted lines represent two extreme cases of the pressure dependence of the indirect bandgap of GaP [34].

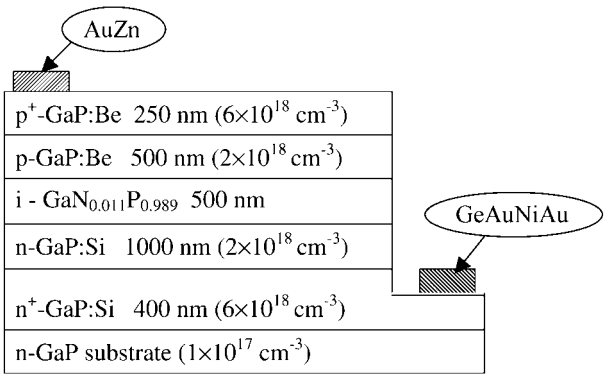

Figure 14. Schematic diagram of a GaNP/GaP LED structure [36].

GaNP is lattice mismatched to GaP, the 500 nm thick GaNP is about 15% strain relaxed, as determined from asymmetric x-ray diffraction. Our recent results on incorporating In into GaInNP show lattice matching and no strain relaxation, so better LED performance can be expected. At present we are fabricating GaInNP/GaP LEDs and the results will be presented elsewhere. The PL intensity of GaNP and GaInNP is comparable to or higher than that of GaInP. Thus, GaInNP/GaP heterostructures are a viable candidate for red high-brightness LEDs, and a single epitaxial growth of LED structures on GaP substrates should be simpler and more cost-effective than the current two-step process of GaAs substrate removal and wafer-bonding to a transparent GaP substrate for high-brightness red LEDs [37].

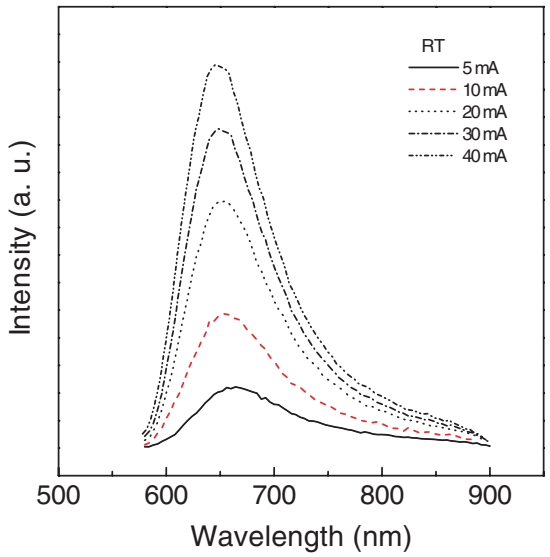

Figure 15. RT electroluminescence at different forward currents of an uncoated DH LED. The inset is the RT PL of the LED sample [36].

6. GaInNP/GaAs(100)

Recently, $Ga_{0.52}In_{0.48}P$ grown lattice matched to GaAs has received considerable attention due to its potential applications in optoelectronic and electronic devices, such as semiconductor lasers [38], HBTs [39] and high-efficiency tandem solar cells [40]. $Ga_{0.52}In_{0.48}P$/GaAs structures have significant advantages over AlGaAs/GaAs structures in larger valence-band discontinuity, better etch selectivity and less oxidation effect.

The conduction-band discontinuity, however, should be eliminated for an npn HBT. Nitrogen incorporation drastically reduces the bandgap energy in $Ga_{1-x}In_xAs$, with the majority of the reduction resulting from lowering of the conduction band, and we expect a similar effect in $Ga_{1-x}In_xN_yP_{1-y}$. Thus, $Ga_{1-x}In_xN_yP_{1-y}$ may be a suitable material for the emitter and collector of an npn HBT, specifically, a blocked-hole HBT [41]. The large valence band discontinuity and large hole effective mass would block holes, while there would be no electron barriers at the base–collector junction. Here we report on the determination of the $Ga_{1-x}In_xN_yP_{1-y}$/GaAs band alignment.

In order to determine the band alignment of $Ga_{1-x}In_xN_yP_{1-y}$/GaAs, a set of eight-period $Ga_{0.46}In_{0.54}N_yP_{1-y}$ (20 nm)/GaAs (5 nm)/$Ga_{0.46}In_{0.54}N_yP_{1-y}$ (20 nm) MQW samples were grown. There is no GaAs QW PL emission when the barrier has a higher nitrogen concentration, such as 1.2% and 2.4%. One possibility is that high nitrogen composition decreases the $Ga_{0.46}In_{0.54}N_yP_{1-y}$ conduction band too much and $Ga_{0.46}In_{0.54}N_yP_{1-y}$/GaAs has a type II alignment, such that the electron and hole separation results in much weaker PL. The PL spectrum of the $Ga_{1-x}In_xN_yP_{1-y}$/GaAs QW having a well thickness of $t_{QW} = 5$ nm taken at 10 K is shown in figure 16. The PL peaks at 1.490 eV and 1.577 eV can be assigned as emissions from the bulk GaAs and the GaAs QW layer itself, respectively. With 0.5% nitrogen incorporation into the $Ga_{1-x}In_xP$ barrier, the position of the GaAs QW PL peak shifts from 1.577 eV to 1.514 eV as shown in figure 16, due to a reduction of the barrier height. Based on the experimental data, the $Ga_{1-x}In_xN_yP_{1-y}$/GaAs band lineup can be calculated using a

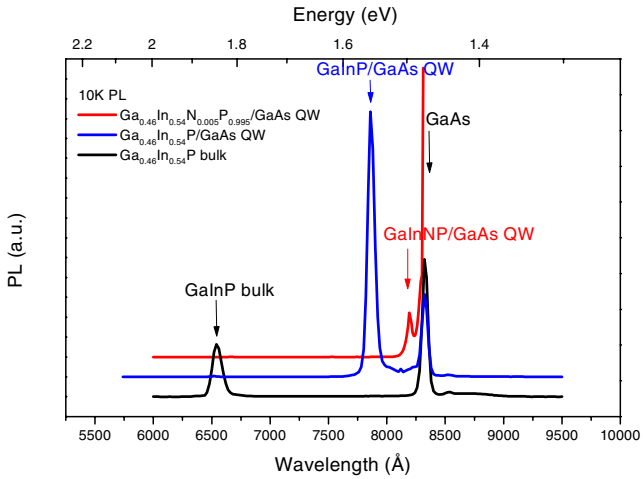

Figure 16. 10 K PL for eight-period $Ga_{1-x}In_xN_yP_{1-y}$/GaAs samples. The well thickness is 5 nm.

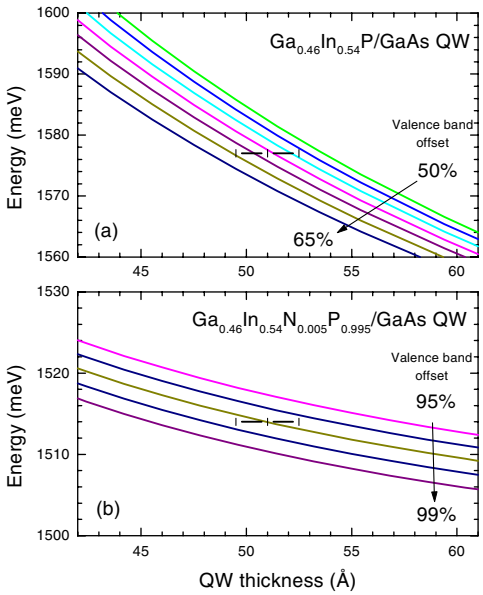

Figure 17. Calculation of transition energy between the first electron and heavy hole confined levels for different values of the valence band offset expressed as a fraction of the total bandgap difference for (a) $Ga_{0.46}In_{0.54}P$/GaAs and (b) $Ga_{0.46}In_{0.54}N_{0.005}P_{0.995}$/GaAs QWs.

finite-barrier quantum well model, where the GaAs electron and hole effective mass at 10 K are 0.067 m_e and 0.51 m_e, respectively [42] (m_e is the free electron mass). The valence band discontinuity fraction α is given by $\Delta E_v/(E_g(\text{GaInNP}) - E_g(\text{GaAs}))$. Figure 17 shows the first quantum confined transition against well thickness with different α. The nominal well thickness 5 nm is confirmed by x-ray simulation within an error bar of one monolayer.

The conduction band and valence band discontinuity value ΔE_c and ΔE_v for $Ga_{0.46}In_{0.54}P$/GaAs are determined to be (42±3) and (58±3)% of the total bandgap difference

(404 meV), respectively, as shown in figure 17(a). This result is similar to previous reports based on the C–V profile method [43, 44]. With 0.5% nitrogen incorporation into $Ga_{0.46}In_{0.54}P$ barrier, ΔE_c and ΔE_v become (3±1) and (97±1)% of total bandgap difference (204 meV), respectively, as shown in figure 17(b). The band reduction mostly happens in the conduction band moving to lower energy, which is similar to nitrogen incorporation in GaInAs [45]. This situation of small ΔE_c but large ΔE_v is ideal for $Ga_{0.46}In_{0.54}N_{0.005}P_{0.995}$ to be the emitter or the collector of an HBT.

At present we are fabricating GaInP/GaAs HBTs with a thin GaInNP hole-blocking layer in the collector, and the results shall be presented elsewhere.

7. Conclusion

Nitrogen incorporation in III–V compounds grown on GaAs, InP or GaP substrates has been investigated. A small amount of nitrogen can has dramatic effects on physical properties: bandgap narrowing, change in the conduction band offset, and even change of the band structure from indirect to direct bandgap as in GaNP/GaP. These characteristics allow many interesting applications. Red GaNP/GaP LEDs are grown and fabricated on transparent GaP substrates. This is a simpler process than removing absorbing GaAs substrates and wafer bonding to GaP substrates. The small bandgap GaInNAs is used as the base of an HBT, which exhibits a lower turn-on voltage, suitable for low-power applications. The bandgap reduction occurs mainly in lowering of the conduction band edge. When N-containing material is in a quantum well, the conduction band offset is increased, resulting in a deeper quantum well and better electron confinement, as in InNAsP/InP and GaInNAs/GaAs. The characteristic temperature of InNAsP/InP microdisc lasers is shown to be 97 K, higher than the conventional GaInAsP/InP lasers. On the other hand, when the N-containing material is in the larger-bandgap material, the conduction band offset is decreased, as in $Ga_{0.46}In_{0.54}N_{0.005}P_{0.995}$/GaAs, which could be an ideal material for npn HBTs.

Acknowledgments

This work is partially supported by the Midwest Research Institute under subcontract No AAD-9-18668-7 from the National Renewable Energy Laboratory, the DARPA Heterogeneous Optoelectronic Technology Center, Army Research Office, Rockwell International and the UC MICRO Program. We gratefully acknowledge the work done by W G Bi, H P Xin, Y G Hong, M Sopanen, R André, R J Welty and fruitful collaborations with Professor P M Asbeck of UCSD, Professor S T Ho of Northwestern University, Y Zhang and A Mascarenhas of the National Renewable Energy Laboratory, and W Shan and W Walukiewicz of the Lawrence Berkeley Laboratory.

References

[1] Weyer M, Sato M and Ando H 1992 *Japan. J. Appl. Phys.* **31** L853
[2] Kondow M, Uomi K, Niwa A, Kitatani T, Watahiki S and Yazawa Y 1995 *Proc. Solid State Device Materials (Osaka)* p 1016
[3] Pearsall T P (ed) 1982 *GaInAsP Alloy Semiconductors* (New York: Wiley)
[4] Zah C-E *et al* 1994 *IEEE J. Quantum Electron.* **30** 511–22
[5] Anan T, Yamada M, Tokutome K and Sugou S 1997 *Electron. Lett.* **33** 1048–9
[6] Kondow K, Nakatsuka S, Kitatani T, Yazawa Y and Okai M 1996 *Japan. J. Appl. Phys.* **35** 5711
[7] Choquette K D, Klem J F, Fischer A J, Blum O, Allerman A A, Fritz I J, Kurtz S R, Breiland W G, Sieg R, Geib K M, Scott J W and Naone R L 2000 *Electron. Lett.* **36** 1388–90

[8] Steinle G, Riechert H and Egorov A Y 2001 *Electron. Lett.* **37** 93–5
[9] Tu C W, Bi W G, Ma Y, Zhang J P, Wang L W and Ho S T 1998 *IEEE J. Sel. Topics Quantum Electron.* **4** 510–3
[10] Ho I-H and Stringfellow G B 1997 *J. Cryst. Growth* **178** 1–7
[11] Bi W G and Tu C W 1996 *J. Appl. Phys.* **80** 1934–2936
[12] Bi W G and Tu C W 1996 *Appl. Phys. Lett.* **69** 3710–12
[13] Bi W G and Tu C W 1997 *Appl. Phys. Lett.* **70** 1608–10
[14] Van Vechten J A 1969 *Phys. Rev.* **182** 891
[15] Sakai S, Ueta Y and Terauchi Y 1993 *Japan. J. Appl. Phys.* **32** 4413–17
[16] Zuo S L, Bi W G, Tu C W and Yu E T 1998 *J. Vac. Sci. Technol.* B **16** 2395–8
[17] Bi W G, Ma Y, Zhang J P, Wang L W, Ho S T and Tu C W 1997 *IEEE Photon. Technol. Lett.* **9** 1072–4
[18] Xin H P and Tu C W 1998 *Appl. Phys. Lett.* **72** 2442–4
[19] Huffaker D L, Park G, Zou Z, Shchekin O B and Deppe D G 1998 *Appl. Phys. Lett.* **73** 2564–6
[20] Anan T, Nishi K, Sugou S, Yamada M, Tokutome K and Gomyo A 1998 *Electron. Lett.* **34** 2127
[21] Yamada M, Anan T, Tokutome K, Nishi K, Gomyo A and Sugou S 1998 *Conf. Prof. LEOS* p 149
[22] Dowd P, Braun W, Smith D J, Ryu C M, Guo C-Z, Chen S L, Koelle U, Johnson S R and Zhang Y-H 1999 *Appl. Phys. Lett.* **75** 1267–9
[23] Xin H P, Kavanagh K L, Kondow M and Tu C W 1999 *J. Cryst. Growth* **202** 419–22
[24] Sopanen M, Xin H P and Tu C W 2000 *Appl. Phys. Lett.* **76** 994–6
[25] Welty R J, Xin H P, Mochizuki K, Tu C W and Asbeck P M 2000 *58th DRC. Conf Digest* (Piscataway: IEEE) p 145
[26] Shan W, Walukiewicz W, Ager J W, Haller E E, Geisz J F, Friedman D J, Olson J M and Kurtz S R 1999 *Phys. Rev. Lett.* **82** 1221–4
[27] Bellaiche L, Wei S H and Zunger A 1997 *Phys. Rev.* B **56** 10 233
[28] Xin H P, Tu C W, Zhang Y and Mascarenhas A 2000 *Appl. Phys. Lett.* **76** 1267–9
[29] Thomas D G, Hopfield J J and Frosch C J 1965 *Phys. Rev. Lett.* **15** 857
[30] Thomas D G and Hopfield J J 1966 *Phys. Rev.* **150** 680
[31] Groves W O, Herzog A H and Craford M G 1971 *Appl. Phys. Lett.* **19** 184
[32] Baillargeon J N, Chen K Y, Holfl G E, Pearah P J and Hsieh K C 1992 *Appl. Phys. Lett.* **60** 2540–2
[33] Zhang Y, Mascarenhas A, Xin H P and Tu C W 2000 *Phys. Rev.* B **61** 4433
[34] Shan W, Walukiewicz W, Yu K M, Wu J Q, Ager J W III, Haller E E, Xin H P and Tu C W 2000 *Appl. Phys. Lett.* **76** 3251
[35] Xin H P, Welty R J and Tu C W 2000 *Appl. Phys. Lett.* **77** 1946
[36] Xin H P, Welty R J and Tu C W 2000 *IEEE Photon. Technol. Lett.* **12** 960
[37] Kish F A and Fletcher R M 1997 *High Brightness Light Emitting Diodes* ed G B Stringfellow and M G Craford (New York: Academic) p 196
[38] Liau Z L, Palmateer S C, Groves S H, Walpole S H, Walpole J N and Missagia L J 1992 *Appl. Phys. Lett.* **60** 6–8
[39] Ahmari D A, Raghaven G, Hartmann, Q J, Hattendorf M L, Peng M and Stillman G E 1999 *IEEE Trans. Electron. Dev.* **46** 634
[40] Bertness K A, Kurtz S R, Friedman D J, Kibbler A E and Olson J M 1994 *Appl. Phys. Lett.* **65** 989–91
[41] Welty R J, Hong Y G, Xin H P, Tu C W, Asbeck P M and Mochizuki K 2000 *Proc. IEEE/Cornell Conf. on High Performance Devices* (Piscataway: IEEE) pp 33–40
[42] Shur M 1990 *Physics of Semiconductor Devices* (Englewood Cliffs, NJ: Prentice-Hall) p 625
[43] Rao M A, Caine E J, Kroemer H, Long S I and Babic D I 1987 *J. Appl. Phys.* **61** 643
[44] Watanabe M O and Ohba Y 1987 *Appl. Phys. Lett.* **50** 906–8
[45] Zunger A 1999 *Phys. Status Solidi* b **216** 117